

Effect of Soil-Structure Interaction on Vulnerability Function for Reinforced Concrete Structure Building

T. Morii, J. Miyakoshi & K. Yoshida

Institute of Technology, Shimizu Corporation, Tokyo, Japan

N. Toyama

Non-Life Insurance Rating Organization of Japan, Tokyo, Japan



SUMMARY:

When the estimation of earthquake damage of buildings is performed, the vulnerability function which was determined by the data base of damaged buildings during the 1995 Hyogo-Ken Nanbu Earthquake is often used in Japan. However, in some cases, the employed vulnerability function isn't consistent with the building damage caused by the earthquakes occurred in recent years. In this paper, the effects of soil-structure interaction and periodic characteristics of earthquake motion on vulnerability functions in reinforced concrete structure buildings are examined. It is pointed out from our study that the response reduction effects due to the soil-structure interaction become remarkable in the medium-rise buildings such as 8-story when input seismic motion is predominant in the short period.

Keywords: Vulnerability Function, Soil-Structure Interaction, Reinforced Concrete Structure Building

1. INTRODUCTION

When the estimation of earthquake damage of buildings is performed, the vulnerability function which was determined by the data base of damaged buildings during the 1995 Hyogo-Ken Nanbu Earthquake is often used in Japan. However, in some cases, the employed vulnerability function isn't consistent with the building damage caused by the earthquakes occurred in recent years. This inconsistency may come from the differences in ground motion characteristics and seismic performance of buildings, and response reduction effects due to the soil-structure interaction, etc. Vulnerability functions are also estimated from the results of earthquake response analyses by using the fixed-base model. It is known that this estimation method is practically useful for examining the building damage ratios considering characteristics of structure performance, ductility capacity, and seismic ground motions (Miyakoshi et al., 2005). In this paper, response reduction effects due to the soil-structure interaction are taken into account to this method, and then the effects of soil-structure interaction on vulnerability functions used for reinforced concrete structure buildings are examined. In the published papers, the effects of soil-structure interaction on earthquake responses of buildings were studied based on relations between actual seismic damage of buildings and observed earthquake motions (Yasui et al., 1998, Takahashi and Hayashi, 2004). However, the effects of soil-structure interaction on vulnerability functions have not been summarized systematically.

In order to construct a simple estimation method which can evaluate responses of buildings considering soil-structure interaction effects, parametric studies on earthquake response analyses are carried out using both the fixed-base model and sway-rocking models. Next, by considering ratios of responses obtained by the sway-rocking models to those by the fixed-base model, we examine the effects of soil-structure interaction on the dynamic responses of reinforced concrete structure buildings. Some parameters sensitive to the response reduction effects are selected from the statistical analyses of the response ratios. Periodic characteristics of input ground motions, the number of stories and seismic performance of buildings are chosen to construct the simple estimation method in this study. Finally, we examine the response reduction effects due to the soil-structure interaction and periodic characteristics of input ground motions for vulnerability functions in reinforced concrete structure buildings. The proposed simple estimation method is compatible with the previous one to evaluate vulnerability functions.

2. CALCULATION METHOD FOR VULNERABILITY FUNCTION

Figure 1 shows the flowchart of calculation method for vulnerability functions based on the results of earthquake response analyses (Miyakoshi et al., 2005). First, earthquake response analyses are performed by using the fixed-base model in this method. The seismic performance of buildings and PGV levels of input ground motions are selected analysis parameters. Next, occurrence probabilities of damage are calculated from the maximum drift angle R_{fix} using criteria for estimation of damage, and then damage ratios are obtained from the results of multiplying the probabilities by the distributions of base shear coefficient C_y . Finally, the vulnerability function of specific building model is estimated by calculating for various PGV levels. In this paper, response reduction effects due to the soil-structure interaction are taken into account to this method. The vulnerability function in consideration of soil-structure interaction effects is created from maximum drift angle R_{sr} in the sway-rocking (SR) model. R_{sr} is estimated to multiply R_{fix} by the evaluation model of response ratio R_{sr}/R_{fix} . The response ratios R_{sr}/R_{fix} are constructed from the results of this study in Section 5.

3. SEISMIC RESPONSE ANALYSIS CONSIDERING SOIL-STRUCTURE INTERACTION

3.1. Outline of analysis model

General outline of seismic response analyses considering soil-structure interaction effects is depicted in Figure 2. In this paper, to take account of soil-structure interaction effects, SR model is employed. First of all, seismic response analyses of subsurface soil models are carried out to obtain the foundation input motions and physical properties of the subsurface soil considering the nonlinearity. Foundation input motions are defined as response waves at the bottom of foundations in the subsurface soil models. When seismic response analyses of SR models are performed, the obtained foundation input motions are used as input motions for the analyses of buildings. Next, dynamic soil stiffness and damping for SR models are calculated based on the physical properties (S-wave velocity and damping) of the subsurface soil. Finally, maximum drift angle R_{sr} is computed from the results of seismic response analyses of SR models by using foundation input motions. On the other hand, the seismic response analyses of the fixed-base model are carried out by using the foundation input motions at the ground surface.

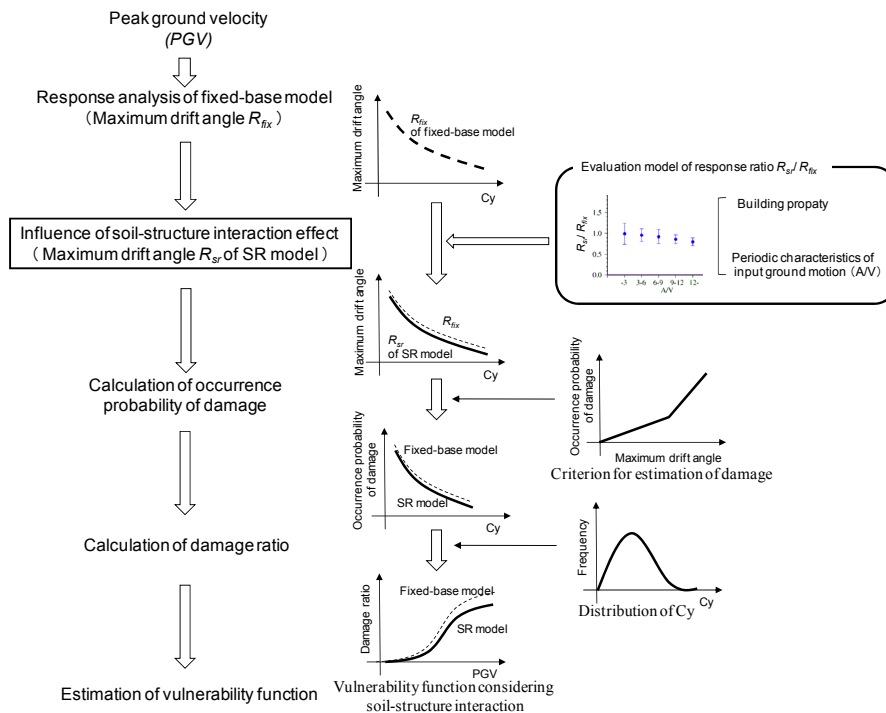


Figure 1. Flowchart of calculation method for vulnerability functions considering soil-structure interaction

From the results of earthquake response analyses, the ratio of R_{sr} to the maximum drift angle R_{fix} of fixed base model is defined as the response ratio R_{sr}/R_{fix} .

The initial equivalent S-wave velocity V_{se} , elastic natural period T_{so} , soil type are selected as analysis parameters in subsurface soil models. The building models are assumed to be reinforced concrete structures, whose parameters are the number of stories N , seismic performance defined as the base shear coefficient C_y , configuration of foundation (area A and aspect ratio BC of foundation), and embedment depth, as listed in Table 1.

3.2. Foundation input motion and shear-wave velocity

To obtain the S-wave velocity considering the nonlinearity of soil, seismic response analyses of subsurface soil models are performed by using the method of SHAKE (Schenabel et al, 1972). Input motions for the subsurface soil models are employed artificial waves with random phase numbers, and are fitted to the acceleration response design spectrum as illustrated in Figure 3. They are normalized by the maximum velocity V . The maximum velocity is assumed to be from 20 to 80cm/s at 20cm/s intervals. The density ρ and Poisson's ratio of soil are uniformly 1.8g/cm^3 and 0.45, respectively. The S-wave velocity V_{sB} of bedrock is set to 400m/s. The elastic natural periods T_{so} of subsurface soil models are ranging from 0.25 to 1.0s, and they are corresponding to the initial equivalent S-wave velocity from 100 to 300m/s. Two types of soil, sand and clay, are used in the analyses and the nonlinear characteristics of soil are employed as shown in Figure 4 proposed by Koyamada et al. (2003). When the embedment depth is 0m or the fixed base model, 2E wave at the ground surface is used as the foundation input motions. In other cases, E+F wave at the bottom of foundation is used for seismic response analyses of buildings.

3.3. Dynamic soil stiffness and damping

Dynamic impedance functions are calculated using the obtained S-wave velocity in consideration of nonlinearity of the subsurface soil. The axisymmetric finite element method(FEM), as depicted in Figure 5, is employed for calculation. An energy transmitting boundary at the side and a viscous boundary at the bottom of the FEM domain are used. The impedance functions are evaluated in the center position of foundation model, and foundations are assumed to be rigid. In the present study, the impedance functions are calculated up to 10Hz in order to cover natural periods of building models. The constant stiffness and damping coefficient are used for SR models, soil stiffness is obtained from the static value in real part of impedance functions, damping coefficient is obtained by the average value up to 10Hz in imaginary part, as illustrated in Figure 6.

3.4. Estimation of maximum drift angle

In the present study, we focus on reinforced concrete (RC) structure buildings. Seismic response

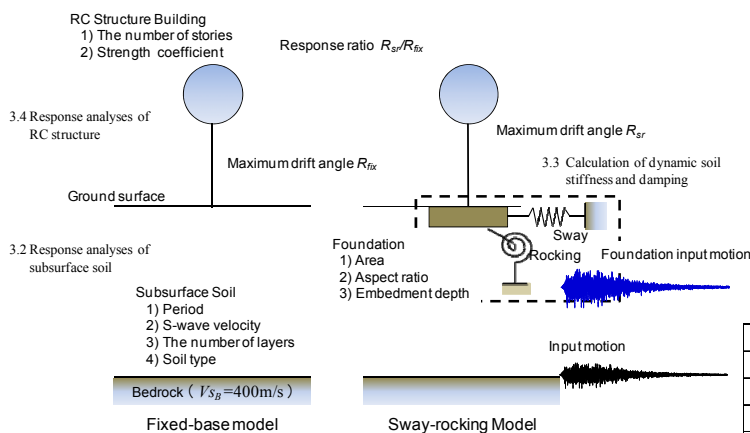


Figure 2. General outline of analysis models

Table 1. Parameters of soil models and RC structure buildings

(a) Subsurface soil model				
Elastic natural period $T_{so}(s)$	0.25, 0.5, 0.75, 1.0			
Initial equivalent S-wave velocity $V_{se}(m/s)$	100, 150, 200, 250, 300			
The number of layers	1, 2, 4			
Soil Type	Sand, Clay			
(b) RC structure building model				
The number of stories N	2	4	8	15
Strength coefficient α	2, 3, 5			
Area $A (m^2)$	50, 100, 150	200, 400, 900		
Aspect ratio BC	1, 3			
Embedment depth $D (m)$	0, 3	3, 6, 10		

analyses in consideration of soil-structure interaction are carried out by using the multi-degree-of-freedom system. The following method is used for RC structure building models. For example, the analysis model of 4 story RC building is shown in Figure 7. Figure 8 indicates the relations between the base shear coefficient C_y and natural period T_{b0} (the number of stories N). Takeda model is used as the hysteretic characteristics of RC structures. The yield drift angle R_y is defined at $1/150\text{rad}$, yield shear force Q_y is calculated from $Q_y = C_y Mg$, where M and g are the total mass and the gravitational constant, respectively. The first break point is calculated from primary shear force $Q_y/3$ and stiffness, which is obtained from the natural period T_{b0} . The base shear coefficient C_y of RC structure is defined as $C_y = \alpha / N$, where α is the strength coefficient. The weight and height of each story are assumed as uniform, weight per unit area is $1(\text{t}/\text{m}^2)$, and height of story is $3(\text{m})$. The building height is $H_b = 3.0N$, and natural period T_{b0} of RC structure is denoted by $T_{b0} = 0.02H_b$. Stiffness distribution of building is considered as trapezoid distribution, whose ratio of the highest floor to the first floor is 0.5, and story shear coefficient distribution follow as A_i distribution. In the case of $\alpha = 3-5$, assumed relations between C_y and T_{b0} correspond approximately to the investigation results in the past damage earthquake.

4. EFFECT OF SOIL-STRUCTURE INTERACTION ON SEISMIC RESPONSE

In order to construct a simple estimation method which can evaluate responses of buildings considering soil-structure interaction effects from those neglecting the effects, parametric studies on earthquake response analyses are carried out using both the fixed-base model and the sway-rocking models. From the results of the earthquake response analyses of RC structures in consideration of soil-structure interaction effects, we examine the influence of analysis parameters on the maximum drift angle and response ratio.

4.1. Relations between seismic intensity index and maximum drift angle

Figure 9 shows the relations between the maximum drift angle R_{fix} of fixed-base model and the peak

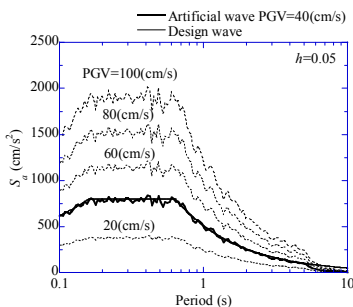


Figure 3. Input motions for subsurface soil model

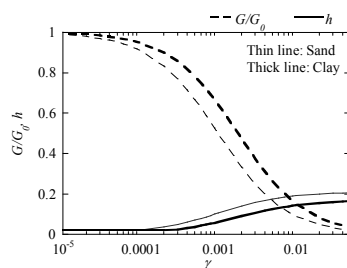


Figure 4. Nonlinear characteristics of subsurface soil

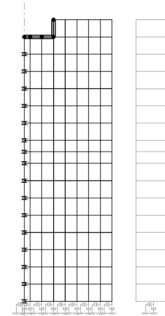


Figure 5. Analysis model for axisymmetric FEM

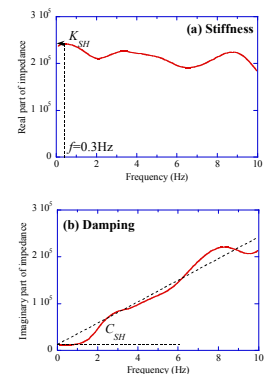
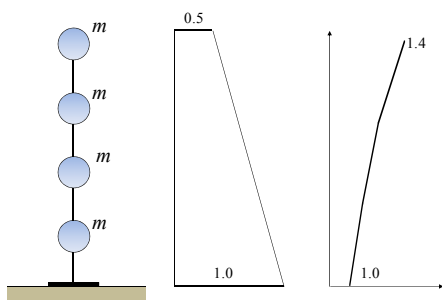


Figure 6. Calculating method of the constant value



(a) Stiffness (b) Strength (c) Hysteretic characteristics

Figure 7. Analysis model of 4-story RC structure building

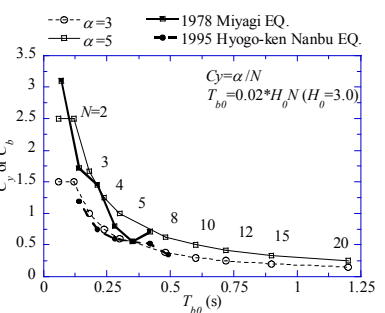
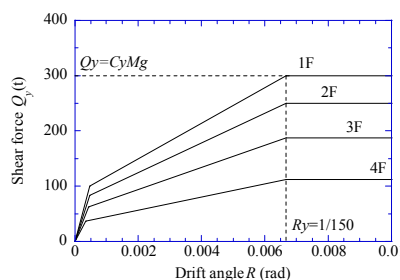


Figure 8. Relations between C_y and T_{b0}

ground velocity (PGV). This figure indicates the results for various stories N when the strength coefficient $\alpha=3$. The maximum drift angle R_{fix} is increasing as PGV becomes large, and the periodic characteristics A/V of foundation input motions, which effects greatly on R_{fix} , is changing due to the number of stories. R_{fix} becomes large when the building model has 4 stories and the foundation input motions are predominant in the short period such as periodic characteristic A/V is more than 6. On the other hand, R_{fix} becomes large in the A/V less than 6, in the case of medium and high-rise buildings such as $N=8,15$.

4.2. Analysis indices for response ratio

Next, we study the analysis indices used for the response ratio. Various response ratios R_{sr}/R_{fix} are plotted in Figure 10 against characteristics of ground motions and maximum drift angles. This figure shows the results of 8 story model. From this figure, since the values of R_{sr}/R_{fix} are uniformly distributed for the PGV of foundation input motions, it is clear that there are few relations between R_{sr}/R_{fix} and PGV . As for the maximum drift angle R_{fix} , R_{sr}/R_{fix} becomes slightly small in range from 0.005 to 0.01rad of R_{fix} . On the other hand, R_{sr}/R_{fix} seems to be affected more A/V than PGV or R_{fix} . Then, the response ratio R_{sr}/R_{fix} is analyzed by using the periodic characteristic T_{ge}/T_{b0} , which is normalized the converted period $T_{ge}(2\pi/(A/V))$ of foundation input motion by natural period T_{b0} of building. When T_{ge}/T_{b0} is around 2, the response ratio R_{sr}/R_{fix} becomes more than 1 due to the soil-structure interaction effects. As T_{ge}/T_{b0} is far from 2, the response ratio R_{sr}/R_{fix} becomes less than 1, maximum drift angle is decreasing. However, when T_{ge}/T_{b0} is more than 5, the response ratio R_{sr}/R_{fix} becomes large again, but R_{fix} is very small in that case. Hereafter, the response ratio R_{sr}/R_{fix} is examined in detail by using T_{ge}/T_{b0} .

4.3. Influence of analysis parameters on the response ratio

4.3.1. Seismic performance, Area and aspect ratio, Embedment depth

Figure 11 shows the influence of analysis parameters on the response ratio R_{sr}/R_{fix} . This figure shows the results of 8 story model, whose basic parameters are strength coefficient $\alpha=3$, area of foundation $A=400m^2$, aspect ratio $BC=1$, embedment depth $D=3m$. First, the influence of seismic performance on R_{sr}/R_{fix} is shown in Figure 11(a). R_{sr}/R_{fix} becomes small as strength coefficient becomes large. Next, the influence of area A and aspect ratio BC of foundation on R_{sr}/R_{fix} is shown in Figures 11(b), (c).

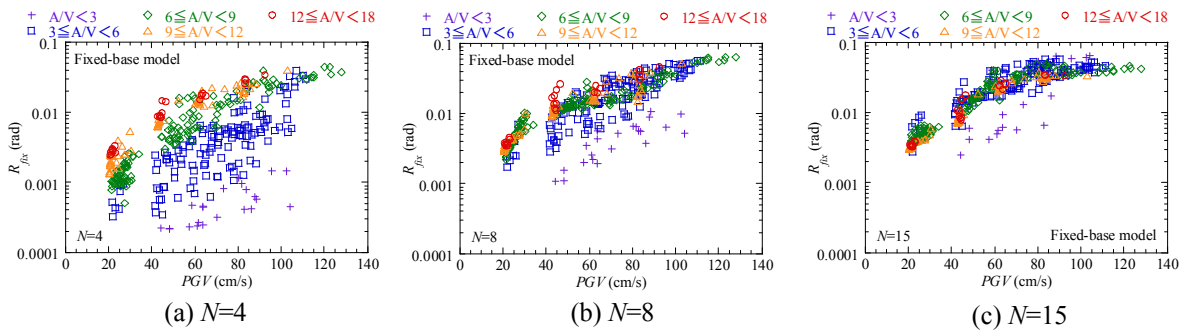


Figure 9. Maximum drift angle R_{fix} of the fixed-base model ($\alpha=3$)

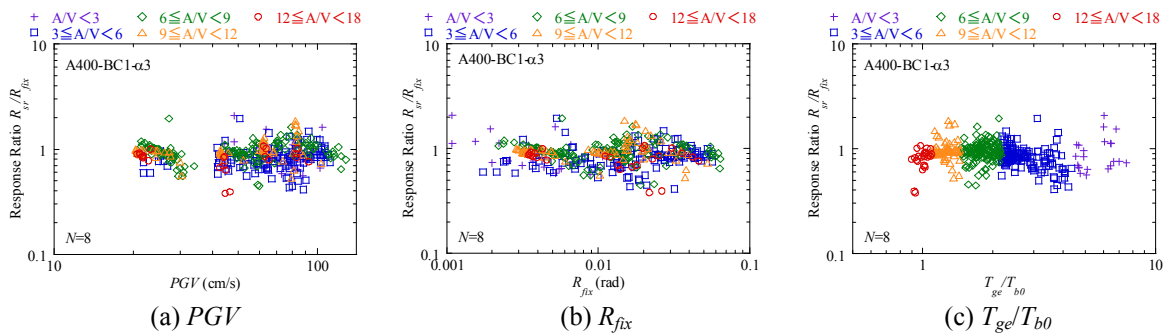


Figure 10. Relations between analysis index and response ratio

R_{sr}/R_{fix} hardly changes with the differences of area or aspect ratio, and the influence of these factors is not so great in the present range. Finally, the influence of embedment depth D is shown in Figure 11(d). R_{sr}/R_{fix} is small as the embedment depth becomes large. Therefore, the reduction of foundation input motions according to embedment depth affects on R_{sr}/R_{fix} greatly.

4.3.2. The number of stories

The influence of the number of stories on R_{sr}/R_{fix} is studied (Figure 11(e)). The area of foundation A is changed depending on the number of stories, $A=100\text{m}^2$ for 4 story, $A=400\text{m}^2$ for 8 story, $A=900\text{m}^2$ for 15 story model, the embedment depth D is 3m in all models. When the embedment depth is the same as $D=3\text{m}$, variations of R_{sr}/R_{fix} due to the number of stories are not so large. However, since natural period T_{b0} alters according to the number of stories, the relations of normalized periodic characteristics T_{ge}/T_{b0} have changed.

4.3.3. Statistical analyses of response ratio

Figure 11(f) shows the results of statistical analyses of R_{sr}/R_{fix} . In the figure, dots denote average value and lines denote average $\pm 1\sigma$. We compare the effects of analysis parameters by using the result of 8 story model mainly. In the comparison of the number of stories, the embedment depth D is assumed 0m in low-rise building models ($N=2,4$), D is assumed 3m in medium and high-rise building models ($N=8,15$). The values of D were determined by the investigation results of existing buildings. It is found from this figure that the influence of area and aspect ratio is not so large, and that the influence of seismic performance, embedment depth and the number of stories is relatively large.

As mentioned above, the analysis parameters which affect response ratios R_{sr}/R_{fix} are the number of stories, seismic performance and embedment depth. Moreover, R_{sr}/R_{fix} alters according to the periodic characteristics of foundation input motions. Therefore, these parameters also need to be taken account when the evaluation model of response ratio is created.

5. ESTIMATION METHOD OF THE RESPONSE RATIO

We propose a simple estimation method which can evaluate responses of buildings considering soil-structure interaction effects from those neglecting the effects. In the simple estimation method, the response ratio R_{sr}/R_{fix} is classified by sensitive parameters such as the number of stories and periodic characteristics of foundation input motions, etc. The periodic characteristics of foundation input motions are expressed by values of A/V . It is known that the maximum drift angle strongly correlates

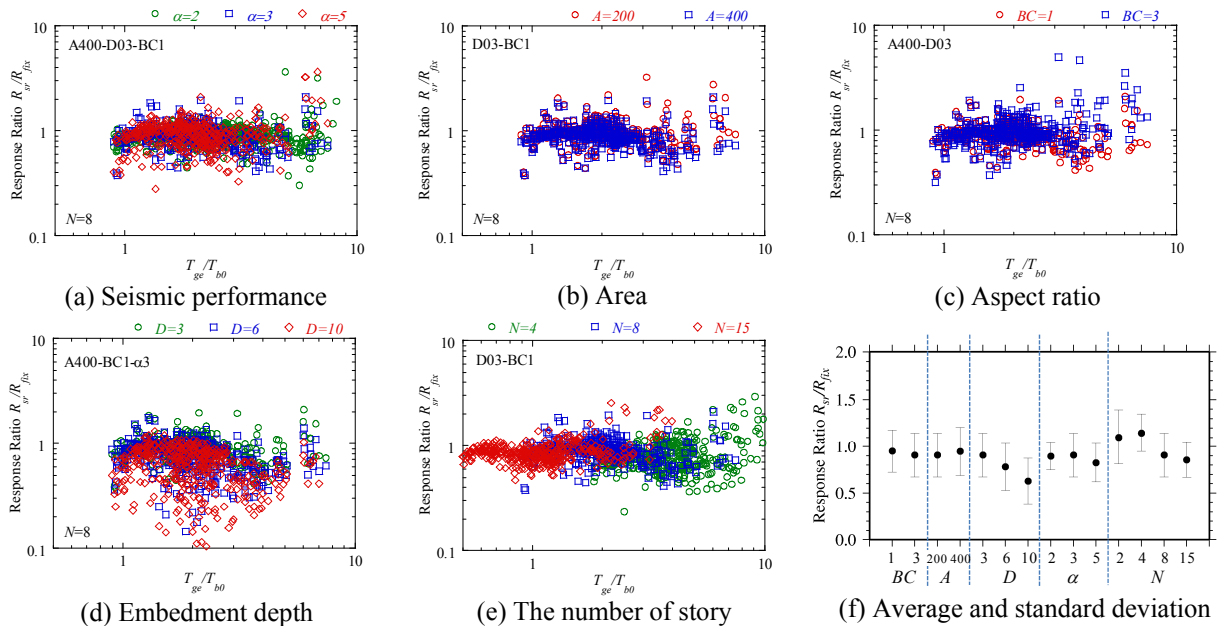


Figure 11. Influence of analysis parameters on response ratio

with damage level. In this paper, we deal with more than 0.005rad of the maximum drift angle, since the response ratio R_{sr}/R_{fix} applies to vulnerability functions.

5.1. Proposed evaluation model of response ratio

Figure 12 shows proposed a simple estimation method of response ratio, which is classified according to the number of stories N , seismic performance α , embedment depth D and periodic characteristics A/V of seismic motion. In the figure, dots denote average value and lines denote average $\pm 1\sigma$ for the result of $\alpha=3$. As previously noted, the embedment depth D is assumed 0m in low-rise buildings ($N=2,4$), D is assumed 3m in medium and high-rise buildings($N=8,15$). The values of A/V of the earthquake motions are sorted out by 4 division such as $3 \leq A/V < 6$, $6 \leq A/V < 9$, $9 \leq A/V < 12$, $12 \leq A/V < 18$. The property of response ratio R_{sr}/R_{fix} differs according to the number of stories. In the case of 2 story model, though variation of R_{sr}/R_{fix} is large, the average value is close to 1, and soil-structure interaction effects are not so large. In the case of 4 story model, R_{sr}/R_{fix} affected by soil-structure interaction when earthquake motion is predominant in the short period such as $12 \leq A/V < 18$. In 8 and 15 stories, R_{sr}/R_{fix} becomes small when the earthquake motions are predominant in the short period.

5.2. Verification of proposed evaluation model due to the observed earthquake motions

Here, we verify the proposed simple method by calculating response ratios using earthquake motions observed in recent years. Table 2 shows the observed earthquake motions. 20 observed earthquake motions are selected for verification from among the main damage earthquakes, which occurred since the 1995 Hyogo-ken Nanbu earthquake, in Japan. The average shear-wave velocity down to 30m from the ground surface ($AVS30$) stands for the ground information on each observation site. On the observation sites in K-NET and KiK-net operated by the National Research Institute for Earth Science and Disaster Prevention (NIED), the values of $AVS30$ are calculated by the information of S-wave velocity opened in the web site. Since the information of S-wave velocity is not clear on other observation sites, the values of $AVS30$ are obtained from the Japan Seismic Hazard Information Station (J-SHIS) by NIED. The relations between the peak ground acceleration PGA and peak ground velocity PGV of observed earthquake motions are shown in Figure 13. The values of PGA are distributed from 200 to 1600 cm/s^2 , the values of PGV are from 20 to 130 cm/s , and the ratios PGA/PGV are from 3 to 18.

Figure 12 compares the proposed response ratio with response ratio calculated by using the observed earthquake motions. In some cases, the simulated response ratios using the observed earthquake motions fall on the outside of average value $\pm 1\sigma$. When the S-wave velocity of subsurface soil is less than 200m/s, the simulated response ratios exceed average value $\pm 1\sigma$ except 8 story building. The reason seems to be that the difference of the spectral characteristics between observed earthquake motions and artificial ground motion increases in the small S-wave velocity. However, on the whole, the simulated response ratios using the observed earthquake motions are contained in the range of average value $\pm 1\sigma$, so these results correspond approximately to the proposed response ratio.

6. VULNERABILITY FUNCTION CONSIDERING SOIL-STRUCTURE INTERACTION AND PERIODIC PROPERTY OF GROUND MOTION

6.1. Calculation of vulnerability function

As shown in Figure 1, the proposed simple method applies to the method of creating vulnerability function. We study the effects of soil-structure interaction on damage ratio of RC structure buildings. Analysis parameters for calculating vulnerability function adduce the same ways of Miyakoshi et al.(2005), as following. In the seismic response analyses of the fixed-base model, the base shear coefficient C_y alters 0.1 to 1.0 at 0.05 intervals, and alters 1.0 to 2.0 at 0.1 intervals. The value of PGV of each observed earthquake motion is changed by 10 cm/s unit in the range from 10 to 200 cm/s . The

Table 2. Used observed earthquake records

Classification of A/V	Site	Earthquake	Dir.	PGA	PGV	PGA/PGV	AVS30	Classification of A/V	Site	Earthquake	Dir.	PGA	PGV	PGA/PGV	AVS30
				(cm/s ²)	(cm/s)							(cm/s ²)	(cm/s)		
3 ≤ A/V < 6	JR Takatori	1995 Hyogo-ken Nambu	EW	657	125	5.3	203	9 ≤ A/V < 12	JMA Kobe	1995 Hyogo-ken Nambu	NS	818	87	9.4	203
	KiK-net Toyokoro	2003 Tokachi Off	EW	404	71	5.7	134		JMA Furukawa	2003 Miyagi Hokubu	EW	213	19	10.9	217
	K-NET Fukuoka	2005 Fukuoka	NS	277	57	4.8	187		K-NET Kushiro	2003 Tokachi Off	EW	407	43	9.6	203
	JMA Wajima	2007 Noto Hanto	EW	439	79	5.5	155		JMA Kawaguchi	2004 Mid Niigata Prefecture	EW	1667	143	11.6	369
	K-NET Kashiwazaki	2007 Niigataken Chuetsu-oki	NS	667	124	5.4	188		JMA Nishiyama	2007 Niigataken Chuetsu-oki	NS	835	76	10.9	308
6 ≤ A/V < 9	JR Takazaka	1995 Hyogo-ken Nambu	EW	601	84	7.2	332	12 ≤ A/V < 18	K-NET Ohno	2001 Geiyo	EW	441	32	14.0	205
	KiK-net Hino	2000 Western Tottori	NS	926	116	8.0	268		JMA Mihara	2001 Geiyo	NS	243	20	12.2	200
	K-NET Anamizu	2007 Noto Hanto	EW	782	100	7.8	136		JMA Kurkoma	2008 Iwate-Miyagi Nairiku	EW	689	53	13.0	316
	JMA Makinohara	2009 Suruga Bay	NS	348	58	6.0	208		KiK-net Ichinosekigashira	2008 Iwate-Miyagi Nairiku	NS	889	63	14.1	434
	K-NET Ishinomaki	2011 off the Pacific coast of Tohoku	NS	458	55	8.4	277		JMA Omaezaki	2009 Suruga Bay	EW	773	47	16.6	380

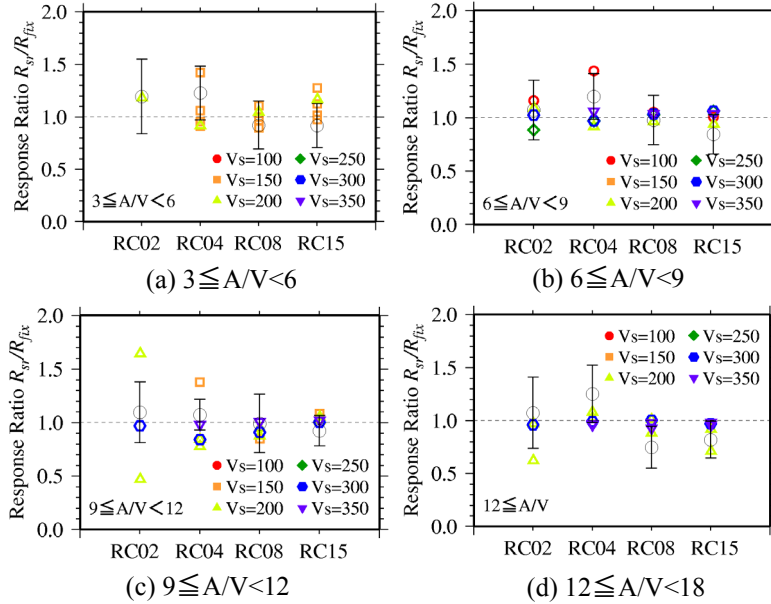


Figure 12. Proposed evaluation model of response ratio ($\alpha=3$)

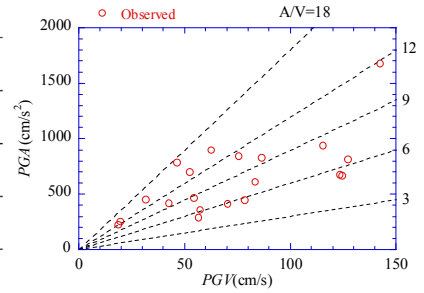


Figure 13. Relations between PGA and PGV of observed ground motion

seismic response analyses of the fixed-base model are performed against total combinations of C_y and PGV . The criteria for estimation of damage and the distributions of C_y are used as shown in Figures 14 and 15. They are configured based on actual earthquake damage during the 1995 Hyogo-Ken Nanbu Earthquake. In this paper, we targeted “complete loss of building” as a damage levels for 4 and 8story buildings. The distributions of C_y are classified depending on the number of stories, 4 story model corresponding to 3-5F division and 8 story building corresponding to 6-10F division. When taking changes of the building response due to the soil-structure interaction effects into consideration, the maximum drift angle of the fixed-base model is multiplied by the response ratio R_{sr}/R_{fix} . Since C_y is set by using the strength coefficient $\alpha=2,3,5$, the response ratios are not consecutive against C_y in the evaluation model. Therefore, when the evaluation model of response ratio applies to the calculation method of vulnerability function, the response ratio interpolates by using Table 3. For example, in 4 story model, the response ratio of $\alpha=2$ is used for $C_y=0.1-0.6$, $\alpha=3$ for $C_y=0.65-1.0$ and $\alpha=5$ for $C_y=1.1-2.0$.

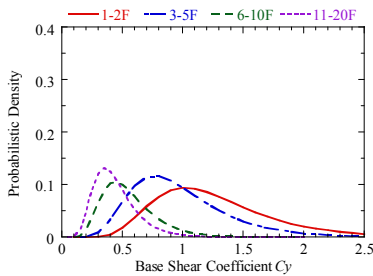


Figure 14. Distributions of base shear coefficient

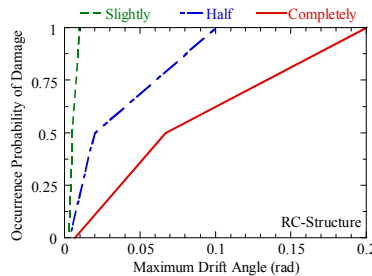


Figure 15. Criteria for estimation of damage

Table 3. Range of response ratio for damage function

The number of stories	Strength coefficient α	Base shear coefficient C_y
$N=2$ (1-2F)	2	0.1-1.3
	3	1.3-1.9
	5	1.9-2.0
$N=4$ (3-5F)	2	0.1-0.6
	3	0.65-1.0
	5	1.1-2.0
$N=8$ (6-10F)	2	0.1-0.35
	3	0.4-0.5
	5	0.55-2.0
$N=15$ (11-20F)	2	0.1-0.2
	3	0.25-0.3
	5	0.35-2.0

6.2. Effect of response ratio on vulnerability function

Seismic response analyses of RC structure buildings are conducted by the method denoted in Section 6.1 and the observed earthquake motions as listed in Table 2. By classification of periodic characteristics A/V , average values of the maximum drift angle are computed, and the vulnerability functions of RC structure buildings are estimated. Figure 16 shows distributions of maximum drift angle for the vulnerability function. In this figure, the results of input level 50cm/s in PGV are shown. Moreover, the vulnerability functions of 4 and 8 story buildings are compared as shown in Figures 17 and 18, respectively. In each figure, the influence of periodic characteristics of earthquake motions and the influence of soil-structure interaction effects are described, comparatively. First, in low-rise buildings ($N=4$), when periodic characteristics A/V become large (earthquake motion is predominant in the short period), damage ratios become large, and difference of damage ratio appears about 15% for 100cm/s (Figure. 17(a)). Even when input levels of earthquake motions are the same, maximum drift angle differs greatly according to the periodic characteristics (Figure. 16(a)). On the other hand, the vulnerability functions are increasing about 3% for 100cm/s in all values of A/V due to the effects of soil-structure interaction (Figure. 17(b),(c)).

Next in medium-rise buildings ($N=8$), although the difference of damage ratio arises until 100cm/s, the difference due to A/V is not so much (Figure. 18(a)). The maximum drift angle becomes almost the same for various values of A/V when the base shear coefficient C_y is low such as less than 0.3. The difference of maximum drift angle affects vulnerability functions only when C_y is high such as more than 0.5 (Figure. 16(b)). As a reason for the influence of A/V becomes small, we presume that the maximum drift angle is not changed so much in medium-rise buildings since building story with the maximum drift angle is changed due to a higher mode. Finally, the effects of soil-structure interaction are examined. Two vulnerability functions are almost the same in $3 \leq A/V < 6$ (Figure.18 (b)). However, The vulnerability function in $12 \leq A/V < 18$ is decreasing about 10% for 100cm/s according to the effects of soil-structure interaction (Figure.18 (c)). As depicted in Figure 16(b), the influence also can be confirmed from variations of the maximum drift angle due to the soil-structure interaction effects.

As mentioned above, when we compare the effects of soil-structure interaction with the effects of periodic characteristic of earthquake motions, the influence changes with the number of stories. The effects of periodic characteristic of earthquake motion become remarkable in the case of low-rise buildings, and the vulnerability functions vary a lot according to this effect. On the other hand, the effects of soil-structure interaction appear greatly in medium-rise buildings when the periodic characteristics of an earthquake motions are predominant in the short period, and damage ratio is decreasing about 10% for 100cm/s.

7. CONCLUSIONS

In this paper, we analyzed effects of soil-structure interaction with periodic characteristics of earthquake motions on vulnerability functions of reinforced concrete structure buildings. The ratio of the maximum drift angle of SR model to that of fixed-base model was defined as the response ratio, and the characteristics of the response ratio were examined for various parameters. We can draw our conclusions as follows.

- 1) Analysis parameters which affect the response ratio are the number of stories, seismic performance and embedment depth. Moreover, the response ratio is also changed by the periodic characteristics of foundation input motions.
- 2) The influence of periodic characteristics of earthquake motions becomes remarkable in the case of low-rise buildings, and the vulnerability functions vary a lot according to the influence.
- 3) The effects of soil-structure interaction appear greatly in medium-rise buildings, when the periodic characteristics of earthquake motions are predominant in the short period, and damage ratio is decreasing about 10% for 100cm/s.

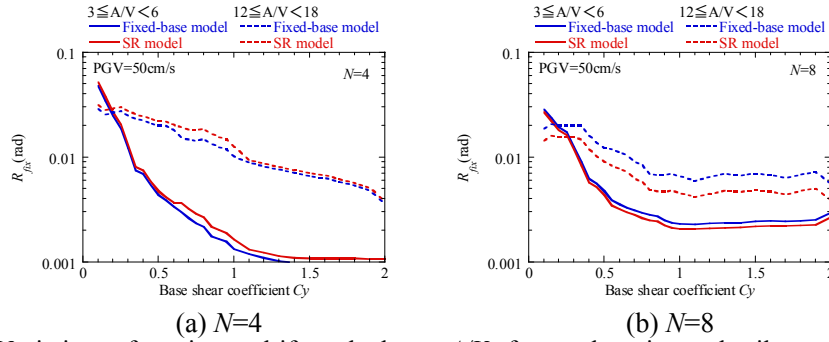


Figure 16. Variations of maximum drift angle due to A/V of ground motion and soil-structure interaction

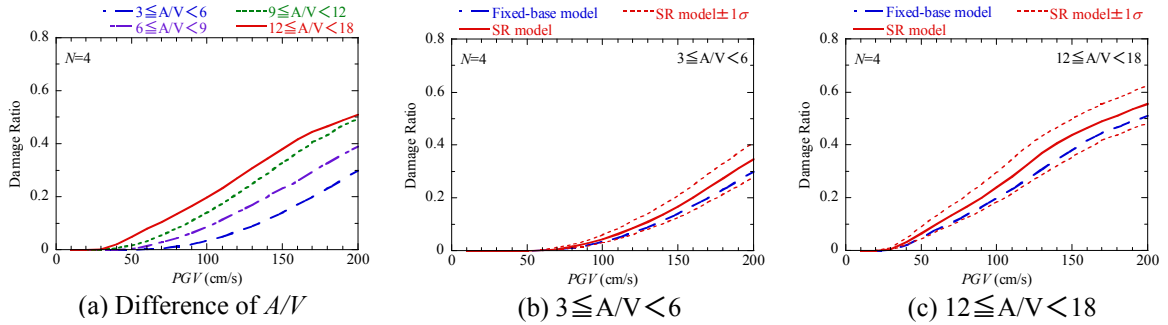


Figure 17. Vulnerability functions for 4-story in RC structure building

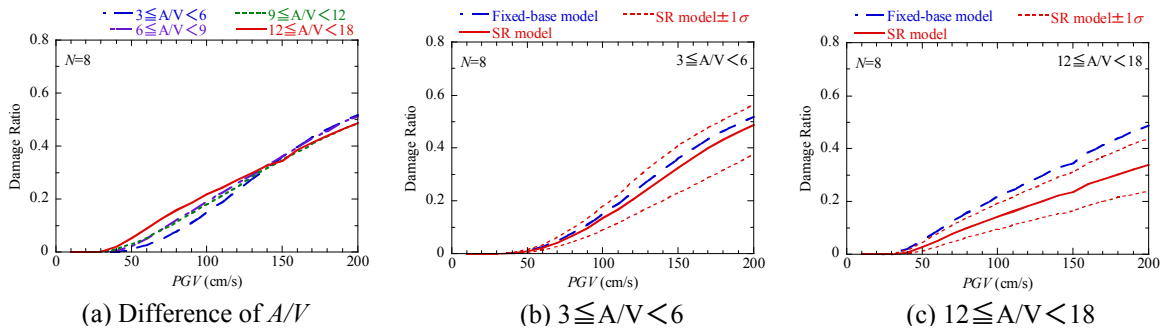


Figure 18. Vulnerability functions for 8-story in RC structure building

ACKNOWLEDGEMENT

This study was performed as a part of the researches supported by the research funding for earthquake insurance operated by Non-Life Insurance Rating Organization of Japan. We used valuable seismic observation records of JMA, K-NET and KiK-net provided by the NIED.

REFERENCES

- Takahashi, I. and Hayashi, Y. (2004). Effectiveness of Soil-Structure Interaction in Earthquake Response Reduction of Buildings. *Journal of Structural Engineering*. **50B**, 1-11(in Japanese).
- Yasui, Y., Iguchi, M., Akagi, H., Hayashi, Y. and Nakamura, M.(1998). Examination on Effective Input Motion to Structures in Heavily Damaged Zone in the 1995 Hyogo-Ken Nanbu Earthquake. *Journal of Structural and Construction Engineering, Transactions of Architectural Institute of Japan*. **512**, 111-118 (in Japanese).
- Miyakoshi, J., Kambara, H., Ishii, D., Tamura, K., Yamaguchi, M., Natori, A. and Yoshimura, M.(2005). Vulnerability Function Based on Earthquake Response Analysis with Dispersion of Structural Strength and Ductility Capacity. *Journal of Structural Engineering*. **51B**, 105-110(in Japanese).
- Koyamada, K., Miyamoto, Y. and Miura K (2003). Nonlinear Property for Surface Strata from Natural Soil Samples, *Workshop of geo-technique, The Japanese geotechnical society*. **38**, 2077-2078(in Japanese).
- P.B.Schenabel, J.Lysmer and H.B.Seed. (1972).SHAKE, A Computer Program for Earthquake Response Analysis of Horizontally Layered Sites, *EERC72-12*.